

2-Deoxy-D-glucose induces deglycosylation of proinflammatory cytokine receptors and strongly reduces immunological responses in mouse models of inflammation

Ikuno Uehara¹ | Mitsuko Kajita¹ | Atsuko Tanimura¹ | Shigeaki Hida² |
Munehiko Onda³ | Zenya Naito³ | Shinsuke Taki⁴ | Nobuyuki Tanaka¹ 

¹Department of Molecular Oncology, Institute for Advanced Medical Sciences, Nippon Medical School, Tokyo, Japan

²Department of Molecular and Cellular Health Sciences, Graduate School of Pharmaceutical Sciences, Nagoya City University, Nagoya, Japan

³Department of Pathology, Integrative Oncological Pathology, Nippon Medical School, Tokyo, Japan

⁴Department of Molecular and Cellular Immunology, Shinshu University School of Medicine, Matsumoto, Japan

Correspondence

Nobuyuki Tanaka, Department of Molecular Oncology, Institute for Advanced Medical Sciences, Nippon Medical School, Sendagi 1-1-5, Bunkyo-ku, Tokyo 113-8602, Japan.
Email: nobuta@nms.ac.jp

Funding information

No funding bodies had any role in study design, data collection and analysis, decision to publish, or preparation of the manuscript.

Abstract

Anti-proinflammatory cytokine therapies against interleukin (IL)-6, tumor necrosis factor (TNF)- α , and IL-1 are major advancements in treating inflammatory diseases, especially rheumatoid arthritis. Such therapies are mainly performed by injection of antibodies against cytokines or cytokine receptors. We initially found that the glycolytic inhibitor 2-deoxy-D-glucose (2-DG), a simple monosaccharide, attenuated cellular responses to IL-6 by inhibiting N-linked glycosylation of the IL-6 receptor gp130. Aglycoforms of gp130 did not bind to IL-6 or activate downstream intracellular signals that included Janus kinases. 2-DG completely inhibited dextran sodium sulfate-induced colitis, a mouse model for inflammatory bowel disease, and alleviated laminarin-induced arthritis in the SKG mouse, an experimental model for human rheumatoid arthritis. These diseases have been shown to be partially dependent on IL-6. We also found that 2-DG inhibited signals for other proinflammatory cytokines such as TNF- α , IL-1 β , and interferon - γ , and accordingly, prevented death by another inflammatory disease, lipopolysaccharide (LPS) shock. Furthermore, 2-DG prevented LPS shock, a model for a cytokine storm, and LPS-induced pulmonary inflammation, a model for acute respiratory distress syndrome of coronavirus disease 2019 (COVID-19). These results suggest that targeted therapies that inhibit cytokine receptor glycosylation are effective for treatment of various inflammatory diseases.

KEYWORDS

2-Deoxy-d-glucose (2-DG), cytokine storm, deglycosylation, inflammatory bowel disease, inflammatory diseases, proinflammatory cytokine receptors, rheumatoid arthritis

Abbreviation: 2-DG, 2-deoxy-D-glucose

This is an open access article under the terms of the Creative Commons Attribution-NonCommercial-NoDerivs License, which permits use and distribution in any medium, provided the original work is properly cited, the use is non-commercial and no modifications or adaptations are made.

© 2022 The Authors. *Pharmacology Research & Perspectives* published by John Wiley & Sons Ltd, British Pharmacological Society and American Society for Pharmacology and Experimental Therapeutics.

1 | INTRODUCTION

Inflammation is an adaptive response caused by harmful stimuli and conditions such as infection and tissue injury. Moreover, it has been suggested that chronic systemic inflammation, which causes various diseases, is caused by homeostatic imbalances in the physiological system.¹ The inflammatory response is orchestrated by proinflammatory cytokines such as **interleukins (IL)-6** and **IL-1 β** , and **tumor necrosis factor (TNF)- α** .² Proinflammatory cytokines are multifunctional proteins that regulate cell death in inflammatory tissues, alter vascular endothelial permeability, recruit immune cells, and induce acute phase protein production. During the inflammatory process, tissue-resident and recruited macrophages are activated and secrete various types of chemokines and cytokines to trigger both innate and adaptive immune responses.³ Cytokine signalling is controlled by multiple regulatory checkpoints that include feedback inhibition, which allows tissues to return to an immunological quiescent state. However, dysregulated production of proinflammatory cytokines and their signalling molecules can be detrimental, which causes various human diseases.⁴

The inflammatory response is coordinately regulated by proinflammatory cytokines such as IL-6, IL-1, and TNF- α .² Upregulation of these cytokines has been observed in various chronic inflammatory and autoimmune disorders, and antibody-based therapy against these cytokines have been used to effectively treat various inflammatory diseases.⁵ For example, targeting the IL-6 pathway by an anti-IL-6 antibody, anti-IL-6 receptor antibody, or the soluble form of IL-6 receptor **gp130** has become an effective treatment for various rheumatic diseases, Castleman disease, and cytokine release syndrome, and it is partially effective for treatment of inflammatory bowel diseases (IBD), such as Crohn's disease and ulcerative colitis.⁶ Blocking of TNF- α or **TNF receptor (TNFR)** efficiently prevents the progression of rheumatoid arthritis, psoriasis, ankylosing spondylitis, and IBD.⁷ In IBD, many studies have demonstrated that TNF-targeted therapies inhibit the activation and proliferation of pathological T cells, reduce inflammation, and support restoration of intestinal mucosa.⁸ Blocking IL-1 is also effective to treat rheumatic diseases and highly coexisting inflammatory diseases such as cardiovascular disease and type 2 diabetes.⁹ Despite such effectiveness, cytokine-targeted therapies can have detrimental effects.^{6,7} These effects suggest that the imbalance caused by the suppression of a single cytokine signal in the orchestrated control process by multiple cytokines may lead to adverse effects in the immune system.

A cluster of pneumonia cases of unknown cause occurred in Wuhan, Hubei, China in December 2019.¹⁰ Analysis of respiratory tract samples identified a novel coronavirus termed severe acute respiratory syndrome coronavirus-2 (SARS-CoV-2).¹¹ Patients infected with SARS-CoV-2 developed a syndrome called coronavirus disease 2019 (COVID-19). Some patients develop acute respiratory distress syndrome (ARDS) with progressive respiratory failure due to pulmonary edema caused by cytokine storms.¹² The terms cytokine storm and cytokine release syndrome were originally used to describe acute graft-versus-host disease following allogeneic

BULLET POINT SUMMARY

WHAT IS ALREADY KNOWN

- The glycolysis inhibitor 2-deoxy-D-glucose also acts as an inhibitor of N-linked glycosylation.
- N-linked glycosylation is involved for the stability and the signalling function of the IL-6 receptor gp130.

WHAT DOES THIS STUDY ADD?

- 2-DG alleviated the signs and symptoms of mouse models for inflammatory bowel disease, rheumatoid arthritis, and cytokine storm.
- 2-DG inhibited signals for IL-6 and other proinflammatory cytokines such as TNF- α , IL-1 β , and IFN- γ .

WHAT IS THE CLINICAL SIGNIFICANCE?

- These results suggest that targeted therapies that inhibit cytokine receptor glycosylation are effective for treatment of various inflammatory diseases.

hematopoietic cell transplantation. Recently, these terms have also been applied to a similar syndrome following chimeric antigen receptor T-cell therapy.¹³ Cytokine storms are life-threatening systemic inflammatory syndromes characterized by elevated circulating cytokine levels and hyperactivation of immune cells. These storms can be triggered by pathogens, cancers, autoimmune responses, and various immunomodulatory therapies. Immune hyperactivation occurs after inappropriate triggering of immune responses, massive immune cell activation, increased pathogen burden such as sepsis, and prolonged immune activation. These immune responses induce elevated cytokine production (the cytokine storm), which result in hyperinflammation and multiorgan failure.¹³ The levels of proinflammatory cytokines, which include interleukin (IL)-6, IL-1 β , tumor necrosis factor (TNF)- α , and **interferon (IFN)- γ** , are elevated and are considered to play major immunopathological roles in patients with cytokine storms.

Because acute respiratory failure and sepsis induced by cytokine storms are the main causes of mortality among COVID-19 patients,¹⁴ anti-cytokine therapeutic strategies, which include cytokine neutralization and cytokine receptor blockade, have been applied in patients with severe COVID-19. Treatment of COVID-19 patients with the IL-6 inhibitor **tocilizumab** decreases the risks of intubation and mortality.¹⁵ The utility of antibody drugs that block inflammatory cytokines such as IL-6 is widely acknowledged, and these drugs are administered to patients with various inflammatory diseases such as rheumatoid arthritis.¹⁶ However, in addition to targeting only one cytokine, there are several functional limitations of antibody drugs, which include inadequate pharmacokinetics and tissue accessibility as well as off-target effects on the

immune system.¹⁷ Moreover, high production costs limit the widespread use of antibody drugs.

In the present study, we found that the glycolytic inhibitor 2-deoxy-D-glucose (2-DG), a simple monosaccharide, attenuated cellular responses to IL-6 by inhibiting N-linked glycosylation of the IL-6 receptor gp130.¹⁸ 2-DG also blocked TNF- α , IL-1 β , and IFN- γ signals, and efficiently alleviated a mouse model of inflammatory bowel disease and human rheumatoid arthritis and prevented death following lipopolysaccharide (LPS) shock, a mouse model of a cytokine storm,¹⁹ and attenuated LPS-induced pulmonary inflammatory responses, a mouse model of ARDS.²⁰ Our results show that glycosylation is a new therapeutic target for inflammatory diseases and a new drug target for future treatments of inflammatory diseases.

2 | METHODS

2.1 | Mice

C57BL/6, SKG (CREA Japan, Tokyo, Japan), and *Il-6*^{-/-} mice (The Jackson Laboratory, Bar Harbor, Maine, USA) were used at 6–10 weeks of age. Animal experiments were reviewed by the Ethics Committee on Animal Experiments of Nippon Medical School (Ethics approval numbers 21–185, 22–115, 22–140, 23–022, 23–184, 23–186, 24–049, 24–143, 27–126, and 2020–082). The study was carried out in accordance with the Guidelines for Animal Experiments of Nippon Medical School, the guidelines of the Law and Notification of the Government of Japan and The ARRIVE Guidelines. Mice were maintained in a 12 h light/12 h dark cycle at 20–24°C with 40%–70% humidity. They were housed at a maximum number of five and were provided with free access to laboratory mouse chow (MF; Oriental Yeast Co, Ltd. Tokyo, Japan) and drinking water. All mice were checked for health and stress every day. The animal experiment protocol was approved by the Ethics Committee on Animal Experiments of Nippon Medical School (ethics approval number 26–020, 27–188).

2.2 | Cell culture

Wildtype (WT) MEFs were prepared as described previously.²¹ PECs were prepared 4 days after injection of 2 mL of 3% thioglycollate broth (Becton Dickinson, Franklin Lakes, NJ, USA) by peritoneal lavage with ice-cold phosphate-buffered saline (PBS). Cells were washed twice and used for total RNA preparation or immunoblotting. WT MEFs, PECs, HeLa cells, Tig3 cells, and RAW264 cells were cultured in Dulbecco's modified Eagle's medium (Nissui Pharmaceutical Co., Tokyo, Japan) supplemented with 10% fetal bovine serum and 50 μ g/mL kanamycin (Meiji Seika Pharma, Tokyo, Japan). Human acute monocytic leukemia THP-1 cells (Health Science Research Resources Bank, Osaka, Japan) were cultured in RPMI medium (Nissui Pharmaceutical Co.) supplemented with 5% fetal bovine serum.

2.3 | Antibodies and materials

An anti-gp130 antibody (Merck Life Science, Darmstadt, Germany) was used for immunoprecipitation. Concanavalin A (ConA) agarose (J-Oil Mills Co., Tokyo, Japan) was used for lectin precipitation. An antibody against the F4/80 antigen (1:150; Bio-Rad, Hercules, CA, USA) was used for immunostaining. Antibodies against gp130 (1:1000; Merck Life Science), phospho-JAK1 (1:1000, Tyr 1022/1023/p-JAK1; Cell Signaling Technology, Danvers, MA, USA), JAK1 (1:1000; Merck Life Science), phospho-JAK2 (1:1000; Tyr 1007/1008/p-JAK2; Cell Signaling Technology), JAK2 (1:1000; Merck Life Science), phospho-TYK2 (1:1000; Tyr1054/1055/pTyk2; Cell Signaling Technology), TYK2 (1:500; Santa Cruz Biotechnology, Dallas, TX, USA), phospho-STAT3 (1:1000; Tyr 705/p-STAT3; Cell Signaling Technology), STAT3 (1:1000; Cell Signaling Technology), phospho-STAT1 (1:1000; Tyr 701/p-STAT1; Cell Signaling Technology), STAT1 (1:1000; Santa Cruz Biotechnology), TNFR1 (1:1000; Cell Signaling Technology), IFNGR- α (1:1000; Santa Cruz Biotechnology), α -tubulin (1:1000; Sigma-Aldrich, St. Louis, MO, USA), and β -actin (1:1000; Sigma-Aldrich) were used for immunoblot analyses. Other reagents included 2-DG (Sigma-Aldrich), D-mannose (Sigma-Aldrich), tunicamycin (Sigma-Aldrich), recombinant human IL-6 (PeproTech, Rocky Hill, NJ, USA), soluble IL-6 receptor (sIL-6R, PeproTech), 3-bromopyruvate (Cayman Chemical, Ann Arbor, MI, USA), Lonidamine (Cayman Chemical), LPS (*Escherichia coli* O55:B5, Sigma-Aldrich), mPSL (Tokyo Chemical Industry, Tokyo, Japan), recombinant human TNF- α (PeproTech), recombinant human IL-1 β (PeproTech), and mouse IFN- γ (R&D Systems, Minneapolis, MN, USA). For IL-6 stimulation, MEFs were stimulated with IL-6 and sIL-6R (0.6 μ g/mL each).

2.4 | DSS-induced colitis

DSS with an average molecular weight of 36,000–50,000 Da (MP Biomedicals, Santa Ana, CA, USA) was administered to 8-week-old female C57BL/6 mice at a concentration of 2% (w/v) in drinking water as described previously.²² 2-DG (10 mg/mouse; Sigma-Aldrich) was intraperitoneally (i.p.) injected once a day. Body weight was measured every day. Control mice were treated similarly, but were provided with drinking water without DSS and received i.p. injections of PBS without 2-DG.

2.5 | Laminarin-induced arthritis

Laminarin (30 mg/mouse; Sigma-Aldrich) was injected i.p. once into 8-week-old female SKG mice. The mice were maintained in a specific pathogen-free environment with or without 2-DG in their drinking water.²³ Arthritis scores were determined by weekly inspection in a double-blinded manner and scored as follows: 0, no joint swelling; 0.1, swelling of one finger joint; 0.5, mild swelling of the wrist or ankle; and 1.0, severe swelling of the wrist or ankle. Scores for all fingers and toes, wrists, and ankles were summed for each mouse.

2.6 | LPS-induced endotoxin shock

Eight-week-old C57BL/6 mice were injected i.p. with 2-DG (20 mg/mouse) or PBS. Two hours later, LPS (0.8 mg/mouse; Sigma-Aldrich) was injected i.p. Survival rates were monitored for 4 days. Two days after LPS injection, several mice were sacrificed, and their upper lobes of left lungs were prepared for total RNA preparation.

2.7 | LPS-induced acute lung injury

Six-week-old male C57BL/6 mice were randomly divided into five groups (Mock, LPS, LPS+2DG, LPS+mPSL, and LPS+2DG+mPSL; $n = 3$ mice per group). Mice were injected i.p. with or without 20 mg 2-DG and 100 mg/kg mPSL. Subsequently, the mice were administered intratracheal injections of LPS (10 mg/kg) or physiological saline as described previously.²⁴ 2-DG, mPSL, and PBS i.p. injections were administered every 24 h.

2.8 | Immunoblotting and immunoprecipitation

Cells were lysed in lysis buffer (1% Nonidet P-40, 0.25% sodium deoxycholate, 150 mM NaCl, and 50 mM Tris-HCl, pH 7.5), with 1 mM EDTA, 1 mM NaF, 1 mM sodium orthovanadate, and a protease inhibitor mixture (Nacalai Tesque, Kyoto, Japan). Immunoblotting and immunoprecipitation were performed as described previously.²¹

2.9 | Oligosaccharide and lectin staining

SDS-PAGE was performed as described previously.²¹ Oligosaccharide and lectin staining was performed using a GP Sensor Kit (J-Oil Mills) with biotin-labeled ConA (J-Oil Mills) or wheat germ agglutinin (J-Oil Mills) following the manufacturer's standard protocols.

2.10 | GP-F treatment

Cells were lysed in the lysis buffer described above except at pH 8.6. Treatment with recombinant GP-F (TaKaRa Bio) was performed for 16 h following the manufacturer's protocol.

2.11 | Flow cytometry

THP-1 cells were incubated for 15–18 h with or without 25 mM 2-DG in RPMI medium. Thereafter, 2×10^5 cells were resuspended in 50 μ L of ice-cold PBS and stained using a Fluorokine IL-6/TNF- α kit (R&D Systems) or anti-CD130-fluorescein isothiocyanate (Abcam,

Cambridge, UK) following the manufacturers' protocols. Stained cells were analysed by a FACS Calibur (Becton Dickinson).

2.12 | Histological analysis

In the DSS-induced colitis model, mice were sacrificed after drinking water that contained DSS for 7 days. Their colons were fixed in 10% neutral formalin. Paraffin-embedded sections (3.75 μ m thick) were stained with haematoxylin and eosin (HE) or immunostained with an anti-F4/80 antibody. Leg or ankle joints of SKG mice sectioned 12 weeks after laminarin injection were photographed and fixed in buffered 10% neutral formalin. Paraffin-embedded sections (3.75 μ m thick) were stained with HE. In the LPS-induced endotoxin shock and acute lung inflammation model, mice administered i.p. or intratracheal injections of LPS and were sacrificed after 48 h. Their left lungs were fixed in 4% paraformaldehyde. Paraffin-embedded sections (3.25 μ m thick) were stained with HE or immunostained with the anti-F4/80 antibody.

2.13 | Quantitative real-time PCR

Total RNA was extracted from cultured cells using a Nucleospin RNA Kit (TaKaRa Bio, Shiga, Japan) and from tissues with an RNeasy Kit (Qiagen, Hilden, Germany). Complementary DNA was prepared using a PrimeScript RT Reagent Kit (TaKaRa Bio). Quantitative real-time PCR was performed using TaqMan Probe Mix (Applied Biosystems, Foster City, CA, USA) and the StepOne™ Real-Time PCR system (Applied Biosystems). The reactions were cycled as follows: initial incubation at 95°C for 20 s, followed by 50 cycles of 95°C for 1 s and 60°C for 20 s. Predesigned primer/probe sets were as follows: *β -actin*, Mm00607939_s1; *IL-6*, Mm99999064_m1; *IL-1 β* , Mm00434228_m1; *MCP-1*, Mm00441242_m1; *IP-10*, Mm00445235_m1; *TNF*, Mm00443260_g1; *HP*, Mm00516884_g1; *SAA1*, Mm00656927_g1. For each target, mRNA expression levels were calculated relative to those of *β -actin* in accordance with the manufacturer's protocol.

2.14 | Plasmids

The pStat3 Luc plasmid was obtained from SABiosciences (Frederick, MD, USA). Control plasmids phRL-TK (renilla luciferase reporter) and pNF- κ B Luc have been described previously.²¹

2.15 | Enzyme-linked immunosorbent assay

Peripheral blood samples from mice were collected in tubes and allowed to clot for 2 h at room temperature. Whole blood samples were centrifuged at 2000 \times g at 4°C to obtain sera. A Quantikine mouse IL-6 kit and Quantikine mouse TNF- α kit (R&D Systems) were

used to quantitate serum cytokine levels in accordance with the manufacturer's protocols.

2.16 | Lung wet/dry ratio determination

The lung wet/dry weight ratio was determined to assess pulmonary edema as described previously.²⁴ The posterior lobe of the right lung was collected, and its net weight was recorded. The

lung was then heated for 72 h at 65°C and weighed to determine its dry weight.

2.17 | Statistical analyses

Data were expressed as the mean \pm standard deviation of at least three independent experiments. Statistical analyses of parametric data were performed using GraphPad Prism 7 software (GraphPad

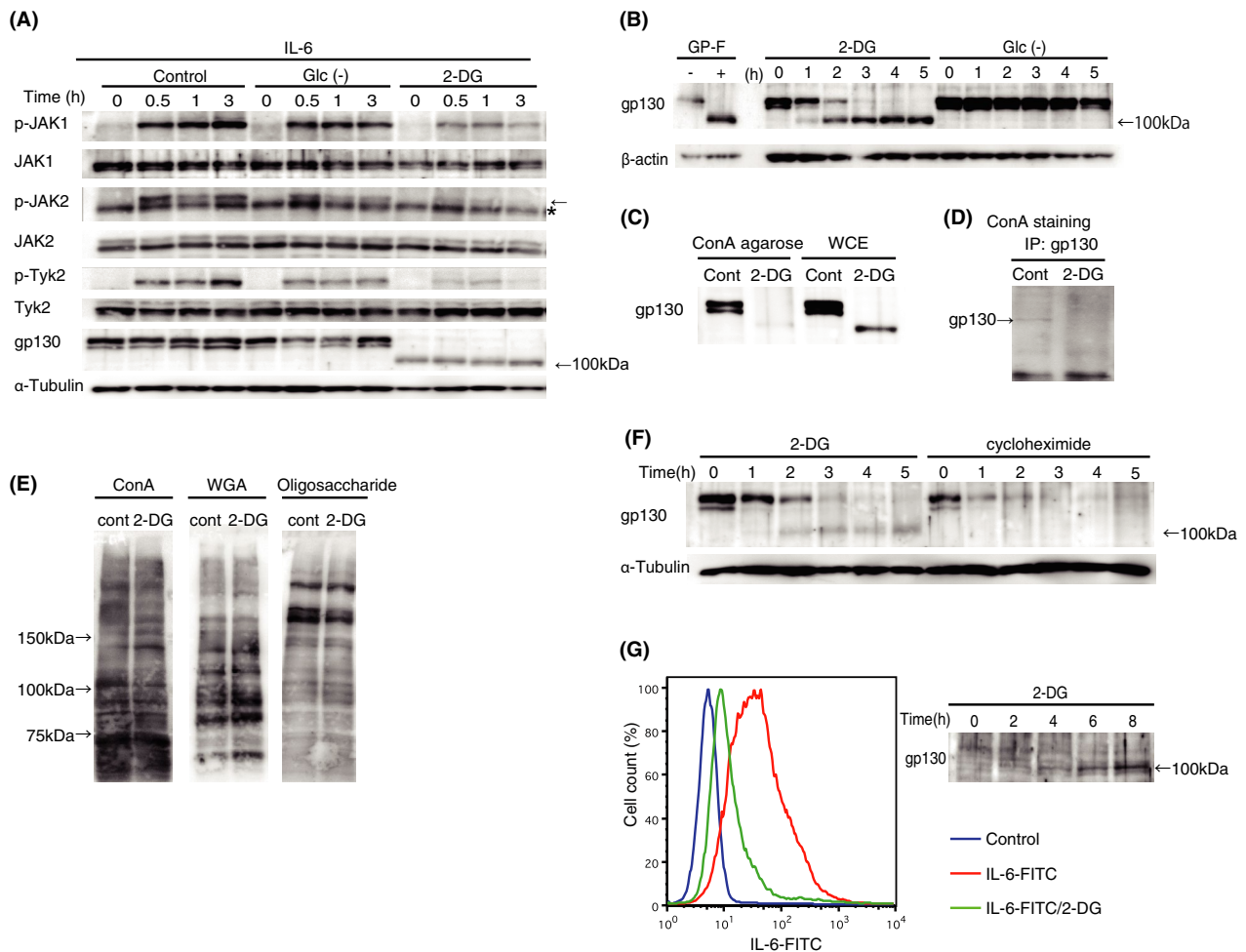
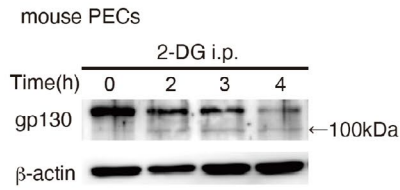
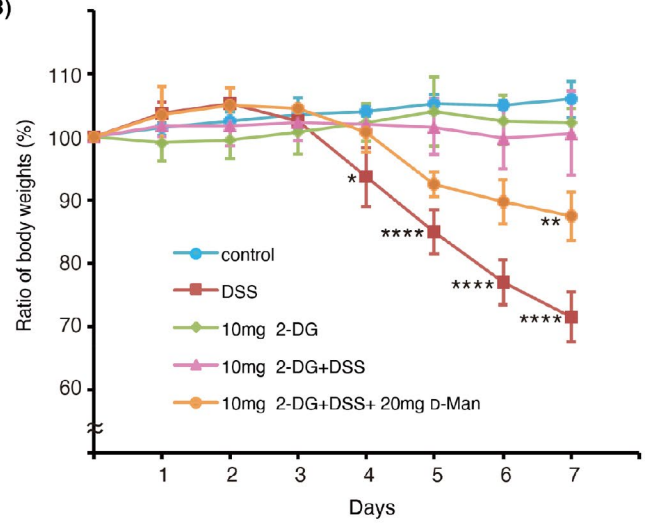


FIGURE 1 2-Deoxy-D-glucose (2-DG) inhibits interleukin (IL)-6 signalling and N-linked glycosylation of its receptor gp130. (A) Wildtype mouse embryonic fibroblasts (MEFs) were incubated in complete medium, glucose-depleted medium (Glc-), or medium with 25 mM 2-DG for 5 h and then stimulated with IL-6 and/or soluble IL-6 receptor (sIL-6R) (0.6 μ g/mL each) for the indicated periods. Activating phosphorylation of Janus kinases (JAK1, JAK2, and TYK2) and expression of gp130 were assessed by immunoblotting. (B) Wildtype MEFs were incubated in medium with 25 mM 2-DG or glucose-depleted medium for the indicated periods. Band shifts of gp130 were assessed by immunoblotting. Glycopeptidase F (GP-F) extract was used as a control for inhibition of N-linked glycosylation. (C) Wildtype MEFs were incubated with or without 25 mM 2-DG for 5 h and whole cell extracts were precipitated with concanavalin A (ConA) agarose. ConA-bound proteins were subjected to immunoblotting with an anti-gp130 antibody. WCE, control whole cell extracts subjected to immunoblot analysis. (D) Wildtype MEFs were incubated with or without 25 mM 2-DG for 5 h and then whole cell extracts were immunoprecipitated with the anti-gp130 antibody and subjected to ConA staining. (E) Wildtype MEFs were incubated with or without 25 mM 2-DG for 5 h and whole cell extracts were subjected to ConA and wheat germ agglutinin (WGA) staining. (F) Wildtype MEFs were incubated in medium with 25 mM 2-DG or 100 μ g/mL cycloheximide for the indicated periods. Expression of gp130 was assessed by immunoblotting. (G) Binding of IL-6 to its receptor in the presence or absence of 2-DG was assessed using FITC-conjugated IL-6 by flow cytometry analysis of human acute monocytic leukemia cells (THP1, left panel). The same cells were subjected to immunoblotting using the anti-gp130 antibody as described in (B)

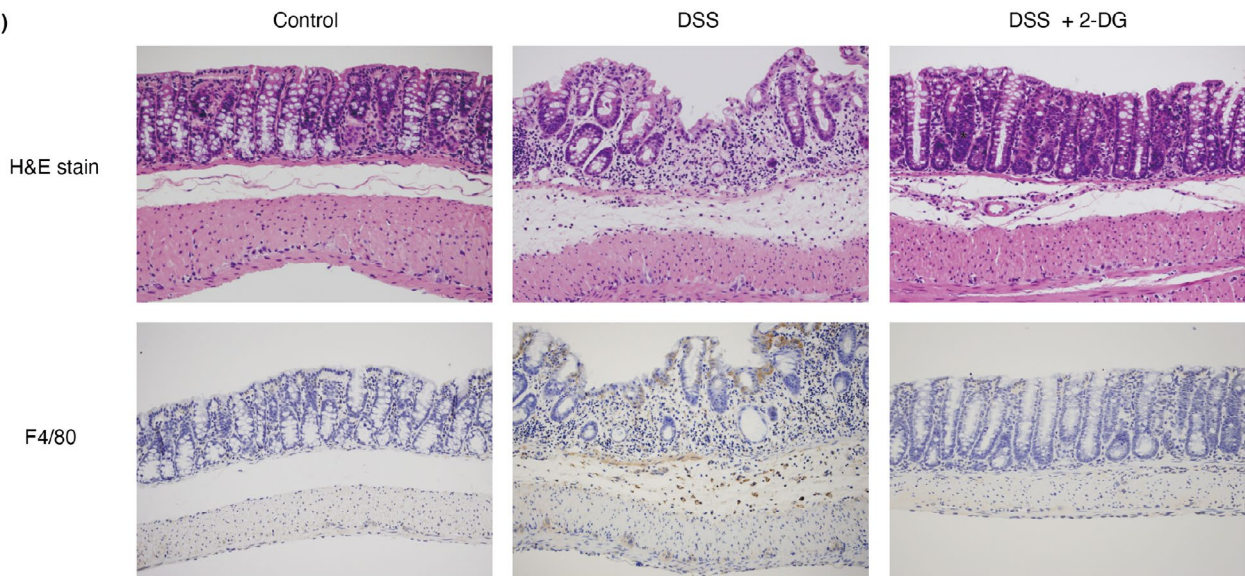
(A)



(B)



(C)



(D)

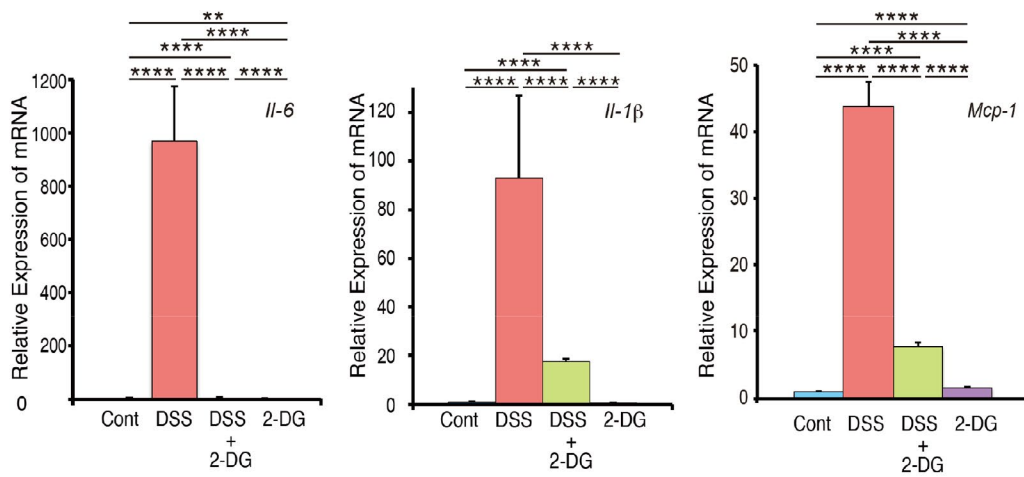


FIGURE 2 2-Deoxy-D-glucose (2-DG) alleviates dextran sodium sulfate (DSS)-induced inflammatory bowel disease. (A) Thioglycollate broth was injected intraperitoneally, and 4 days later, 20 mg 2-DG was injected. Following the injections, mouse peritoneal macrophages were prepared at the indicated times. Expression of gp130 was determined by immunoblotting. (B) Time course of body weight loss. C57BL/6 mice ($n = 4$) were treated with 2% DSS in drinking water with or without 10 mg 2-DG and 20 mg Mannose injections once a day for the indicated periods. Body weight was measured daily. Relative body weight (%) compared with day 0 is plotted with standard errors. Results were analysed using two-way ANOVA followed by Tukey's post hoc test. $*p < .05$ (DSS vs. DSS+2DG 4days), $**p < .01$ (DSS+2DG vs. DSS+2DG +Man 7days) and $****p < .0001$ (DSS vs. DSS+2DG 5,6,7day) were considered statistically significant. Experiments were repeated three times independently with similar results. (C) Histological sections of colon tissues (control, DSS treated for 7 days and DSS+2DG treated for 7 days) following haematoxylin and eosin staining (upper panel, $\times 180$) and anti-F4/80 antibody staining (lower panel, $\times 180$). (D) Quantitative real-time PCR analysis of interleukin (IL)-6, IL-1 β , and haptoglobin (HP) mRNAs in colon tissues of control mice and mice treated with DSS, DSS+2-DG, or 2-DG for 7 days. Results were analyzed using one-way ANOVA followed by Tukey's post hoc test. $****p < .0001$, $**p < .01$. Graphs are presented as the mean \pm s.d. ($n = 3$)

Software Inc.). Significant differences between two groups were determined using the unpaired two-tailed t-test. Multiple comparisons were performed using one-way or two-way analysis of variance (ANOVA) followed by Tukey's post hoc test, unless otherwise stated in the figure legends. The post hoc tests were only conducted when ANOVA results achieved a $p < .05$. For all statistical analyses, $p < .05$ were considered statistically significant unless otherwise indicated.

2.18 | Data availability

The expression profiling microarray data of mouse DSS colitis tissues has been deposited in the GEO database under the accession code GSE167598 available in the GEO repository (<https://www.ncbi.nlm.nih.gov/geo/query/acc.cgi?acc=GSE167598>). All other data that support the findings of this study are available from the corresponding author upon reasonable request.

2.19 | Nomenclature of targets and ligands

Key protein targets and ligands in this article are hyperlinked to corresponding entries in <http://www.guidetopharmacology.org>, the common portal for data from the IUPHAR/BPS Guide to PHARMACOLOGY,²⁵ and are permanently archived in the Concise Guide to PHARMACOLOGY 2019/20.^{26,27}

3 | RESULTS

3.1 | 2-DG inhibits IL-6 signalling and N-linked glycosylation of the IL-6 receptor gp130

IL-6 is a proinflammatory cytokine produced by various myeloid cells, such as macrophages and dendritic cells, in response to a wide range of inflammatory stimuli.¹⁸ IL-6 plays a critical role in initiating and promoting inflammatory responses as shown experimentally in mutant mice that lack IL-6¹⁸ and clinically by the efficacy of IL-6-neutralizing antibodies for treatment of inflammatory diseases.^{28–30} Binding of IL-6 to its receptor, gp130, activates Janus kinases (JAKs) **JAK1**, **JAK2**, and **TYK2**, which subsequently activates their downstream target, **signal**

transducer and activator of transcription 3 (STAT3). Translocation of STAT3 to the nucleus induces the expression of several inflammation-related genes.³¹ Enhanced glucose metabolism plays a major role in oncogenesis.²¹ During our investigations of the role of glucose metabolism in tumor-associated inflammation, we found that JAK activation was suppressed by 2-DG (Figure 1A). Importantly, in mouse embryonic fibroblasts (MEFs) treated with 2-DG, we also found that gp130 expression had disappeared concomitantly with the emergence of an anti-gp130 antibody-reactive protein with a molecular weight of approximately 100 kDa (Figure 1A, bottom). Moreover, glucose starvation did not alter the protein molecular weight or receptor function (activating JAKs in response to IL-6) (Figure 1A), and the hexokinase II inhibitors, 3-bromopyruvate and lonidamine, which inhibit glycolysis, did not induce a molecular weight change of gp130, as shown in 2-DG Figure S1A, suggesting that glycolysis inhibition itself did not cause this change. Considering that gp130 is a glycoprotein with its proteinaceous component having an expected molecular weight of approximately 102 kDa,^{32,33} we hypothesized that the 100 kDa gp130-related protein was an aglycosylated form of gp130. In support of this hypothesis, removal of N-linked oligosaccharides by glycopeptidase F (GP-F)³⁴ resulted in a similar reduction in the gp130 molecular weight (Figure 1B). Furthermore, similar changes in the gp130 molecular weight and inhibition of IL-6 signalling were observed following treatment with tunicamycin,³⁵ an inhibitor of N-linked glycosylation (Figure S1B,C). The inability of this low molecular weight form of gp130 to bind concanavalin A (ConA) in solution (Figure 1C) and on western blots (Figure 1D) further supported its aglycosylated status. In addition to glycolysis-inhibiting activity, 2-DG reportedly inhibits mannose metabolism and mannose-mediated N-linked glycosylation.^{36,37} Metabolome analyses³⁸ showed that glucose-6-phosphate and guanosine diphosphate mannose, a substrate for N-linked glycosylation, had accumulated in 2-DG-treated cells (Figure S2), which suggested that 2-DG inhibited glucose phosphoisomerase and mannosyltransferase.^{37,39} As shown in Figure 1E, global patterns of cellular protein glycosylation were not as dramatically affected by 2-DG treatment compared with gp130 glycosylation as shown by oligosaccharide and lectin staining of whole cell lysates. The gp130 protein has an unusually high turnover rate with a half-life of approximately 2 h,⁴⁰ and its expression had disappeared within a few hours following treatment with the protein synthesis inhibitor cycloheximide. The kinetics were comparable with those of

the molecular weight reduction of gp130 caused by 2-DG treatment (Figure 1F). We speculated that proteins with high turnover rates, such as gp130, were selectively affected by 2-DG. Aglycosylated gp130 appeared to be transported efficiently onto the cell surface, because anti-gp130 antibodies stained 2-DG-treated cells almost as strongly as untreated cells (Figure S3). This observation was inconsistent with a previous report suggesting that N-linked glycosylation of gp130 is important for trafficking to the cell surface.⁴¹ The basis for these discrepant observations remains unclear, but amino acid substitutions in the previous study⁴¹ might have altered the structure of gp130, thereby reducing the efficiency of transportation to the cell surface. Despite normal cell surface trafficking, the IL-6–gp130 association was clearly impaired in 2-DG-treated cells compared with that in untreated cells (Figure 1G). Taken together, these results indicated that 2-DG suppresses IL-6 signalling by inhibiting receptor–cytokine binding, but not the surface expression of gp130. We determined the 2-DG concentration–response and found that a molecular weight change of gp130 induced by 25 mM of 2-DG was still present at 1 mM (Figure S1D).

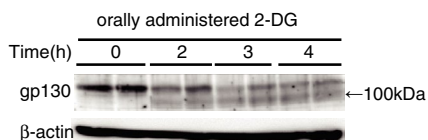
3.2 | 2-DG protects mice from dextran sodium sulfate (DSS)-induced inflammatory bowel disease

Next, we examined the effects of 2DG on IL-6 signalling in mice. Intraperitoneal (i.p.) injection of 2-DG rapidly reduced the molecular weight of gp130 in thioglycollate-elicited peritoneal exudate cells (PECs) (Figure 2A). This finding suggested that 2-DG suppresses inflammation *in vivo* by inhibiting IL-6 responses. To test this hypothesis, we used a series of mouse models of inflammatory diseases. The first was DSS-induced colitis, a mouse model of inflammatory bowel diseases such as Crohn's disease and ulcerative colitis.⁴² Weight loss in mice fed with DSS that received daily injections of 2-DG was dramatically suppressed compared with that in untreated animals, which lost significant weight within 1 week (Figure 2B). Histological analysis of mice that received DSS, but not 2-DG, showed disruption and disappearance of villi and crypts, proliferation of fresh granulation tissue, infiltration of inflammatory cells, and microvascular angiogenesis in

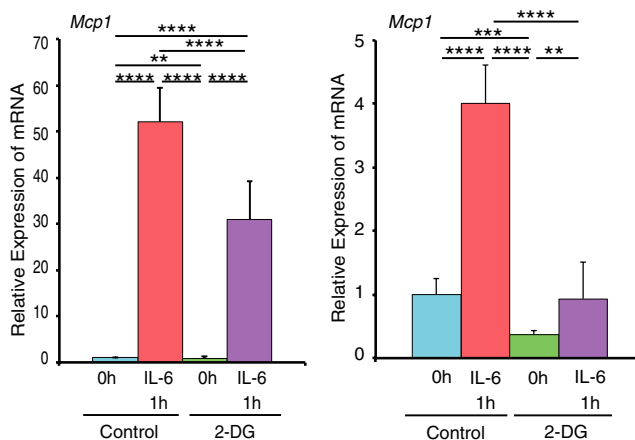
colon tissue (Figure 2C). Conversely, disruption of the colonic lamina propria in mice that received 2-DG treatment was inhibited with much less prominent infiltration by macrophages in the submucosa compared with that in untreated mice. Moreover, slight hyperplasia of crypts was observed in 2-DG-treated mice, which suggested the occurrence of tissue repair (Figure 2C). As expected by the absence of infiltrating macrophages, DSS-induced expression of inflammatory cytokines [IL-6 and IL-1 β produced mainly by activated macrophages and the IL-6 target gene **monocyte chemoattractant protein-1 (MCP-1)**⁴³] was dramatically decreased in 2-DG-treated mice (Figure 2D). Genome-wide expression profiling revealed that DSS-induced upregulation of genes involved in inflammation, which included inflammatory cytokines, chemokines, and proteases,^{44,45} was globally suppressed by 2-DG (Figure S4). Conversely, D-glucosamine, an analog of 2-DG, did not induce deglycosylation of gp130 (Figure S5A compared with Figure 1A) and had no therapeutic effect on DSS-induced colitis (Figure S5B compared with Figure 2B). Moreover, the injection of D-mannose, a substance that counteracts 2-DG inhibition, attenuated the inhibitory effects of 2-DG on gp130 glycosylation and IL-6 signalling in cells (Figure S6A,B) or the *in vivo* effects of 2-DG-induced gp130 deglycosylation as well as suppression of DSS-induced body weight loss and colon tissue disruption (Figure 2B and Figure S7). In addition, D-mannose did not inhibit the 2-DG suppression of adenosine triphosphate production (Figure S6C), which is mainly promoted by glycolysis, suggesting that the inhibition of gp130 glycosylation by 2-DG is mainly caused by the inhibition of mannose-mediated glycosylation, not the inhibition of glycolysis. These results suggested that inhibition of glycosylation, but not of glycolysis, was important for the therapeutic effect of 2-DG on DSS-induced colitis. This hypothesis was supported by the ability of tunicamycin to inhibit DSS-induced disruption of colon tissues (Figure S8). These results indicated that a broad range of macrophage activation signals and macrophage-mediated inflammatory responses were attenuated by 2-DG mediated inhibition of glycosylation. Conversely, a null mutation of the *Il6* gene was far less effective to suppress colitis development than 2-DG treatment (Figure 2B and Figure S9). This led us to speculate that inhibition of IL-6 responses alone could not account for the high therapeutic efficacy and anti-inflammatory activity of 2-DG.

FIGURE 3 2-Deoxy-D-glucose (2-DG) alleviates laminarin-induced arthritis in SKG mice. (A) and (B) C57BL6 mice were injected with thioglycollate broth, and 4 days later, 15 mg/mouse of 2-DG was administered by oral gavage. (A) PECs from two mice at each time prepared at indicated periods after 2-DG administration were subjected to gp130 immunoblotting. (B) MCP-1 mRNA from peritoneal cells and livers of C57BL6 mice injected at 1 h before with 0.5 μ g IL-6/mouse was subjected to quantitative RT-PCR. Results were analysed using one-way ANOVA followed by Tukey's post hoc test. **** p < .0001, *** p < .001, and ** p < .01. (C) Arthritis scores of SKG mice ($n=10$) under specific pathogen-free conditions following a single intraperitoneal injection of 30 mg laminarin with or without 0.5% 2-DG in drinking water. Results were analysed using two-way ANOVA followed by Sidak's post hoc test. * p < .05 (Laminarin 2-DG(-) vs. Laminarin 2-DG(+)) 8 and 9 weeks, ** p < .01 (Laminarin 2-DG(-) vs. Laminarin 2-DG(+)) 7 weeks, and *** p < .001 (Laminarin 2-DG(-) vs. Laminarin 2-DG(+)) 10 weeks were considered statistically significant. n.s.; not significant. Graphs are presented as the mean \pm s.d. ($n = 10$). (D) Growth of mice in (C) was measured via body weight changes. Results were analysed using two-way ANOVA and were not statistically significant. Graphs are presented as the mean \pm s.d. ($n = 10$). (E) Photographs of wrists (upper panel) and ankles (lower panel) of SKG mice 12 weeks after laminarin injection with or without 2-DG treatment. (F) Haematoxylin and eosin staining of ankle joints of SKG mice 12 weeks after laminarin injection as described in (C). (G) Quantitative real-time PCR analysis of haptoglobin (HP) and serum amyloid A (SAA) mRNAs in the liver 12 weeks after laminarin injections as described in (C). Results were analysed using one-way ANOVA followed by Tukey's post hoc test. **** p < .0001. Graphs are presented as the mean \pm s.d. ($n = 3$)

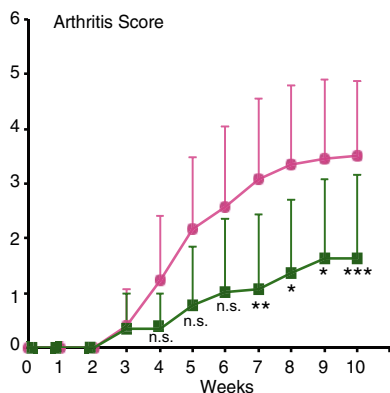
(A) mouse PECs



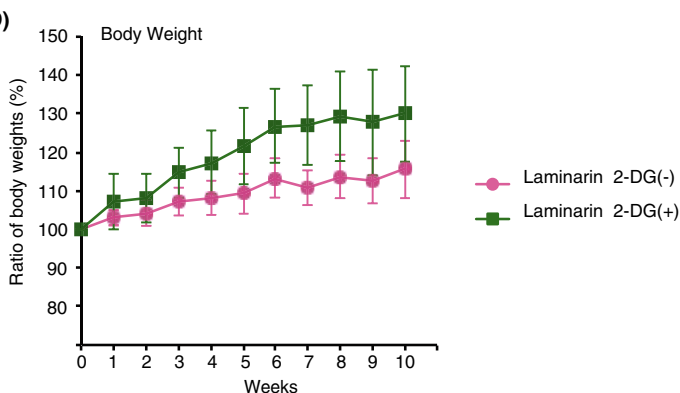
(B) PECs



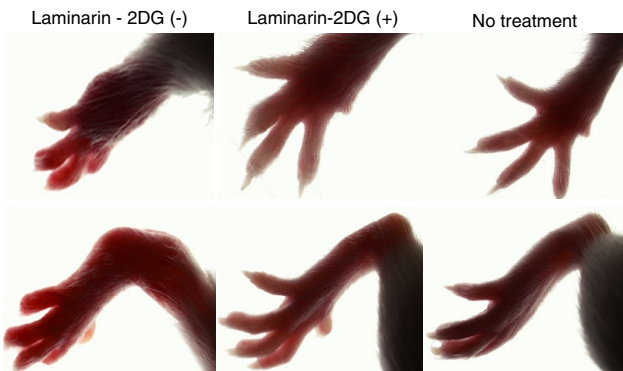
(C) Arthritis Score



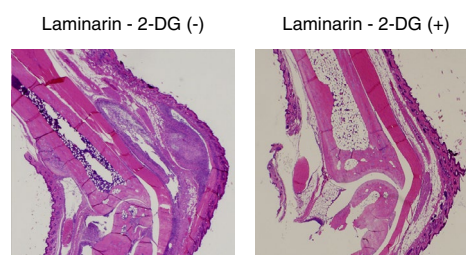
(D) Body Weight



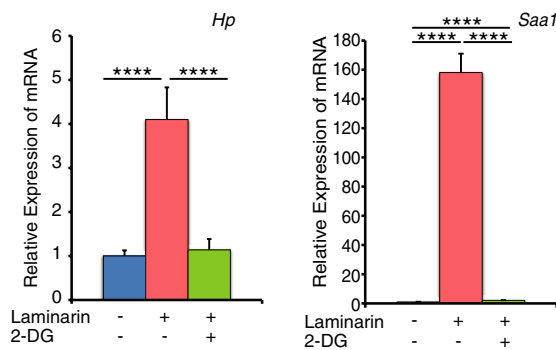
(E)



(F)



(G)



3.3 | Oral 2-DG alleviates laminarin-induced arthritis in SKG MICE

We further examined the effect of orally administered 2-DG on gp130 glycosylation and IL-6 responses *in vivo*. We observed a

similar reduction in the molecular weight of gp130 in PECs isolated from mice administered oral 2-DG to that observed *in vitro* (Figure 3A). Moreover, MCP-1 expression at the mRNA level was upregulated to a lesser extent in PECs and in the liver of mice fed 2-DG that received *i.p.* injection of IL-6 than it was in those of

control mice (Figure 3B). The observation that 2-DG was effective when administered orally implies that 2-DG can be easily administered over long periods of time to treat chronic inflammation. To assess this possibility, we used SKG mice that develop arthritis in a strictly IL-6-dependent manner. IL-1 β and TNF- α are considered as disease-accelerating factors.^{46,47} SKG mice are regarded as an ideal model for human rheumatoid arthritis that is currently treated by injection of protein antagonists of TNF- α , IL-1 β , and IL-6.^{28–30} Oral 2-DG was confirmed to be effective in reducing IL-6 responses in SKG mice *in vivo* (Figure S10). SKG mice developed arthritis at approximately 5 weeks after injection of laminarin,

a β -glucan known to trigger arthritogenic immune responses in these mice (Figure 3C–E).^{46,47} Arthritis severity, as represented by arthritis scores and swollen joints, was clearly reduced in animals administered oral 2-DG compared with that in untreated mice. Accordingly, subsynovial infiltration of macrophages, plasma cells, and lymphocytes was far less prominent in 2-DG-treated mice than in control mice (Figure 3F and Figure S11). The expression of laminarin-induced inflammatory markers haptoglobin (HP)⁴⁸ and serum amyloid A (SAA)⁴⁹ was suppressed in the liver following oral 2-DG administration (Figure 3G). The body weight increase was slower in control SKG mice, likely because of laminarin-induced

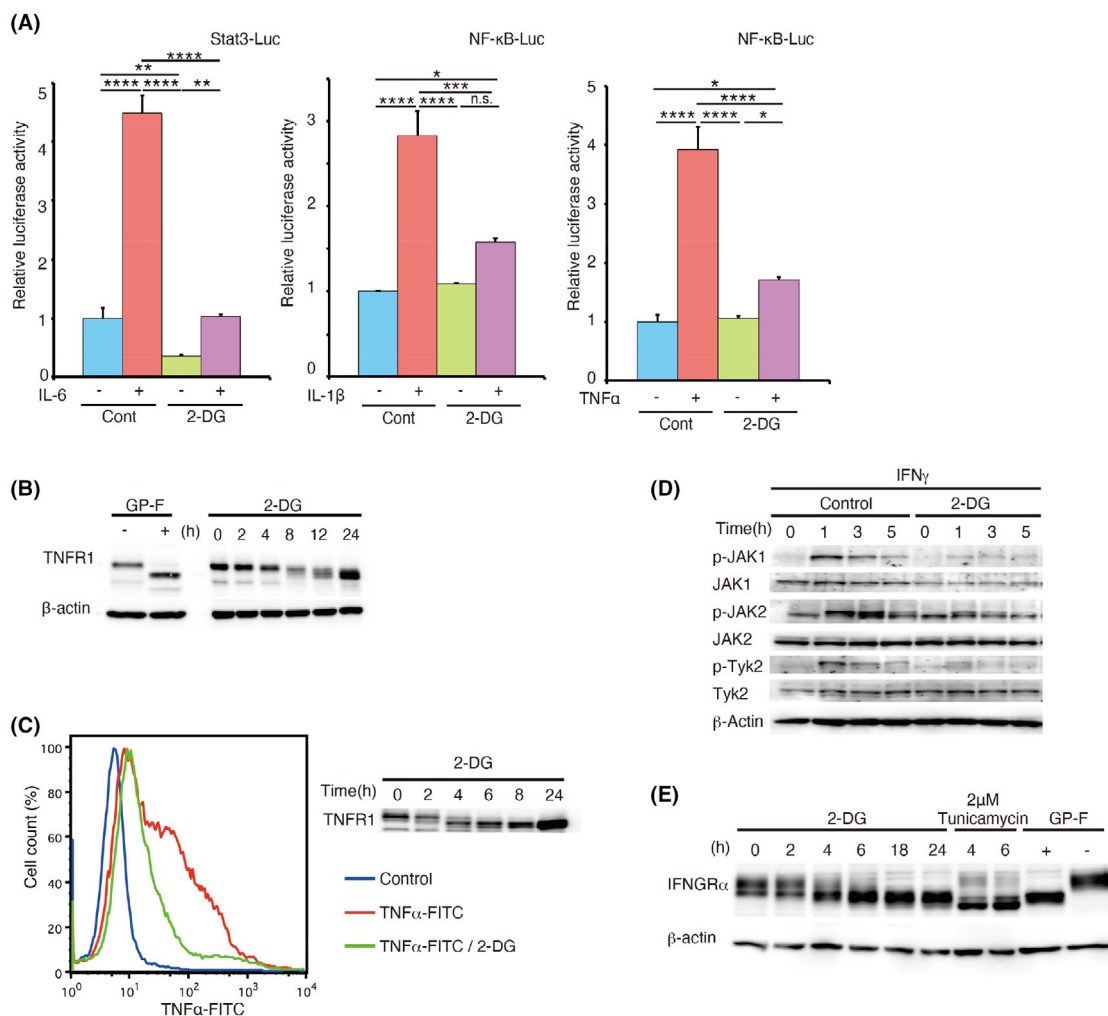


FIGURE 4 2-Deoxy-D-glucose (2-DG) inhibits the functions of tumour necrosis factor (TNF)- α , interleukin (IL)-1 β and interferon (IFN)- γ . (A) HeLa cells were transfected with Stat3 Luc or NF- κ B Luc reporter plasmids or pRL-TK (internal control). After 24 h, cells were treated with or without 25 mM 2-DG for 8 h and then with 0.4 μ g/mL IL-6 with soluble IL-6 receptor (sIL-6R) (Stat3 Luc), 50 ng/mL IL-1 β (NF- κ B Luc), or 100 ng/mL TNF- α (NF- κ B Luc) for 4 h. After stimulation, relative luciferase activity was evaluated. Results were analysed using one-way ANOVA followed by Tukey's post hoc test. **** p < .0001, *** p < .001, ** p < .01 and * p < .05. n.s.; not significant. Graphs are presented as the mean \pm s.d. (n = 3). (B) HeLa cells were incubated in medium with 25 mM 2-DG for the indicated periods. The band shift of TNF receptor 1 (TNFR1) was determined by immunoblotting. Glycopeptidase F (GP-F) extract was used as a control for inhibition of N-linked glycosylation. (C) Binding of TNF- α to its receptor in the presence or absence of 2-DG was determined using FITC-conjugated TNF- α by flow cytometric analysis of THP1 cells (left panel). The same cells were subjected to immunoblotting using an anti-TNFR1 antibody as described in (B). (D) Wildtype mouse embryonic fibroblasts (MEFs) were stimulated with 3000 U/mL IFN- γ for the indicated times. Activating phosphorylation of Janus kinases (JAK1, JAK2, and TYK2) was assessed by immunoblotting. (E) HeLa cells were incubated in medium with 25 mM 2-DG for the indicated periods. Band shift of IFN- γ receptor α -chain (IFNGR α) was assessed by immunoblotting. Tunicamycin and GP-F extracts were used as controls for inhibition of N-linked glycosylation

inflammation. Notably, SKG mice treated with 1% (w/v) 2-DG in drinking water showed consistent increases in body weight over 10 weeks (Figure 3C, right) and no drastic changes in laboratory blood results (Figure S12), which suggested that oral 2-DG was well-tolerated at this dose. The therapeutic efficacy of 2-DG was elevated as doses were increased up to 1%, but no increased efficacy was observed at a dose of 1.5% (Figure S13). At concentrations higher than 2%, water consumption was decreased, making it difficult to achieve a higher dose treatment.

3.4 | 2-DG inhibits responses to TNF- α , IL-1 β , and IFN- γ

In inflammatory diseases, release of inflammatory cytokines leads to activation of immune cells and the production and release of additional cytokines.⁵⁰ Therefore, the *in vivo* therapeutic efficacy of 2-DG for inflammatory bowel disease and arthritis may also involve inhibition of other inflammatory cytokines. We therefore investigated the effects of 2-DG on activation of the transcription factor nuclear factor (NF)- κ B in response to proinflammatory cytokines TNF- α and IL-1 β .⁵¹ Similar to IL-6-induced STAT3 activity, NF- κ B activity induced by TNF- α and IL-1 β was efficiently suppressed by 2-DG (Figure 4A). Notably, 2-DG treatment reduced the apparent molecular weight of the TNFR1 and suppressed ligand binding by the receptor (Figure 4B,C). Activation of JAKs induced by IFN- γ , an important cytokine for macrophage activation during inflammatory responses,⁵² was also inhibited by 2-DG, which was accompanied by a reduction in the molecular weight of IFN- γ receptor α -chain (Figure 4D and E). Additionally, IFN- α/β receptor was deglycosylated by 2-DG, but activation and phosphorylation of JAKs and their target STAT1 were not decreased significantly (Figure S14). Moreover, it has been shown that glycosylation of vascular endothelial growth factor receptor 2 is affected by kifunensine and castanospermine, inhibitors of glycoprotein processing enzyme that convert protein N-linked high mannose carbohydrates to complex oligosaccharides.⁵³ However, castanospermine and another mannosidase inhibitor, 1-deoxymannojirimycin, did not attenuate glycosylation of gp130 and IL-6 signal (Figure S15). These results demonstrated the versatile and specific inhibitory activity of 2-DG against a wide range of proinflammatory cytokine signals, which likely underlies the high therapeutic efficacy of this compound in inflammatory disease models.

3.5 | 2-DG prevents LPS shock and LPS-induced pulmonary inflammatory responses

The above results indicated that 2-DG inhibits multiple cytokine signals, especially inflammatory cytokines involved in cytokine storms. Therefore, we analysed the effects of 2-DG on LPS shock, a mouse model of the cytokine storm.⁵⁴ We found that pretreatment with 2-DG by injection was very effective to prevent death following

LPS shock in mice (Figure 5A) by reducing LPS-induced serum IL-6 and TNF- α production (Figure 5B) as well as mRNA expression of IL-6, IL-1 β , and SAA in the liver (Figure S16). Moreover, i.p. injection of LPS elevated expression of cytokines (TNF- α) and chemokines [MCP-1 and 10 kDa interferon-gamma-induced protein (IP-10)] in the lungs as observed in COVID-19 patients.⁵⁵ Expression of these mRNAs was attenuated by coinjection of 2-DG (Figure 5C). These results suggest that 2-DG attenuates the clinical symptoms caused by cytokine storms. Furthermore, we analysed the effects of 2-DG in LPS-induced acute lung inflammation, a mouse model of ARDS.⁵⁶ As shown in Figure 5D, pulmonary infiltration of inflammatory cells, which included macrophages, was attenuated by coinjection of 2-DG. The same effect was observed by coinjection of a glucocorticoid, methylprednisolone (mPSL), which is now considered the standard of care for patients with severe COVID-19.¹² Furthermore, combined treatment with 2-DG and mPSL completely inhibited pulmonary infiltration (Figure 5D), lung edema (Figure 5E), and expression of MCP-1 and IP-10 in lungs (Figure 5F). These results suggest that targeted therapy with 2-DG to inhibit glycosylation of cytokine receptors alleviates the symptoms of cytokine storms and ARDS.

4 | DISCUSSION

The results of our study suggest that the N-glycosylation of proinflammatory cytokine receptors is an unrecognized potential target for anti-inflammatory therapies. However, there are some disadvantages when using 2-DG, such as toxicity and low pharmacological specificity, which may limit its use for the treatment of inflammatory diseases. At present, it remains unclear why the N-glycosylation of certain surface molecules was inhibited by 2-DG. Similarly, it is unclear which types of proteins, other than the cytokine receptors examined in this study, are affected by 2-DG. It has been shown that the protein half-life of IL-6 receptor gp130 is short.⁵⁷ Because the activity of very short-lived proteins is regulated mainly at the transcriptional level, inflammatory cytokine signals that regulate rapid and transient responses may require the rapid turnover of responsive proteins. Indeed, our results demonstrated that glycosylated forms of IL-6, TNF- α , and IFN- γ receptors rapidly shifted to low molecular weight forms following the administration of 2-DG. On the basis of these results, we think that only a limited number of proteins, such as inflammatory cytokine receptors, may be affected by the once-daily administration of 2-DG, which has a rapid degradation rate. Therefore, although 2-DG has low pharmacological specificity, effects other than its anti-inflammatory properties may not be significant, considering that no serious adverse events were observed in a clinical study,⁵⁸ see the next paragraph) using a human dose equivalent to that used in mice in this study. In addition, we observed that long-term oral administration of 2-DG in mice was well-tolerated. Before 2-DG can be used for the treatment of inflammatory diseases, more detailed *in vivo* analyses of the dose, frequency of administration, and other adverse events of 2-DG are required.

Because nutrient and energy deprivation are considered an efficient method to suppress the growth of cancer cells, whose main energy source is aerobic glycolysis, 2-DG may be an effective anticancer agent.^{59,60} Indeed, many reports have shown that 2-DG suppresses growth and induces apoptosis of cancer cells.⁵⁹ A phase I clinical trial of 2-DG was conducted in patients with advanced solid tumors to evaluate its safety, pharmacokinetics, and maximum tolerated dose. A tolerable dose of 63 mg/kg was identified and

the most significant adverse effects at doses of 63–88 mg/kg were reversible hyperglycaemia (100%), gastrointestinal bleeding (6%), and reversible grade 3 prolongation of the corrected QT interval (22%).⁵⁸ However, the high dosing requirements limited outpatient use and long-term treatment. In the present study, we applied 500–1000 mg/kg 2-DG in mice. The human equivalent dose estimated using average body weights and surface areas, is 40–81 mg/kg.⁶¹ We believe that 2-DG may be beneficial for short-term treatment of

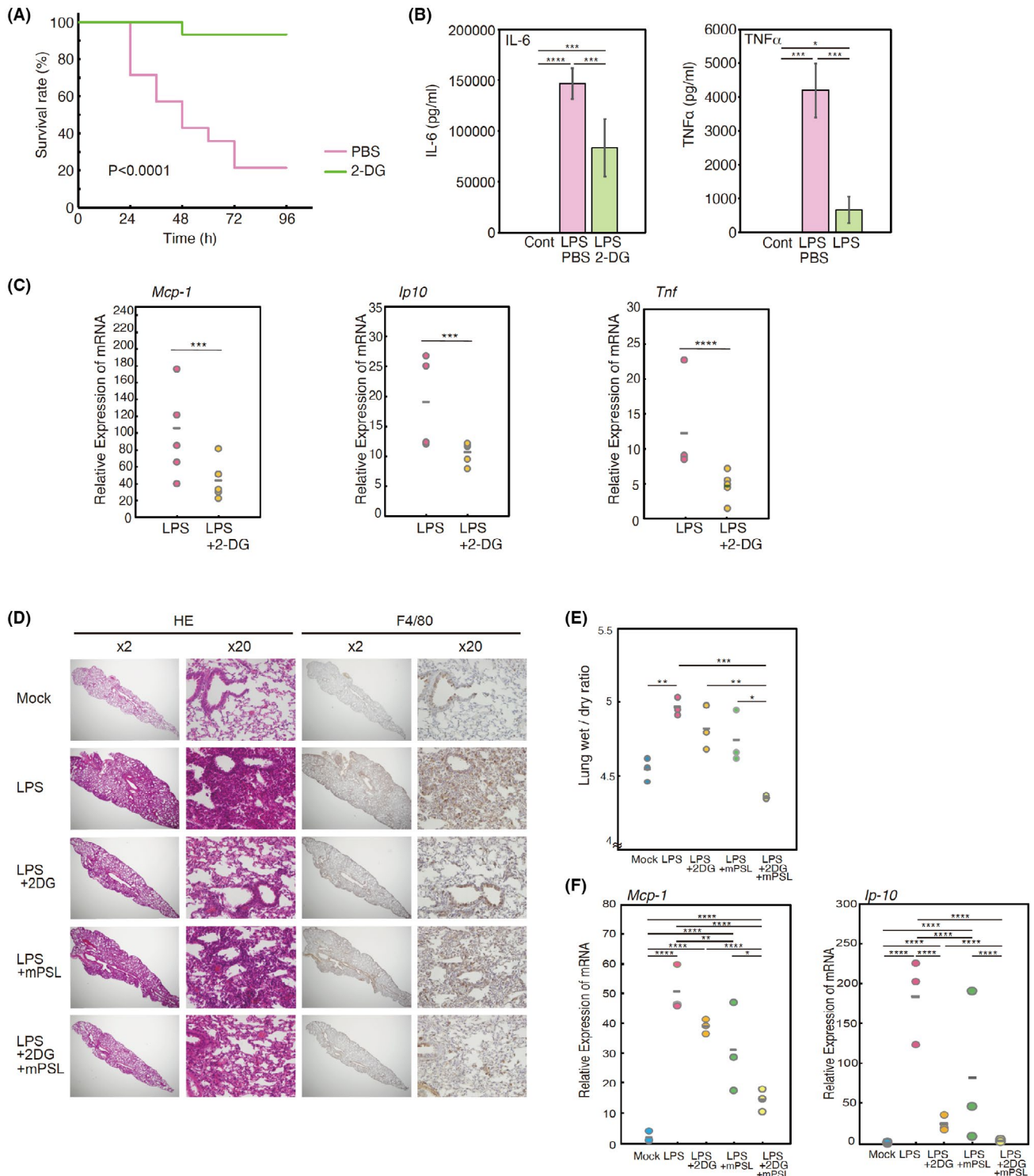


FIGURE 5 2-Deoxy-D-glucose (2-DG) alleviates lipopolysaccharide (LPS)-induced shock and LPS-induced acute lung inflammation. (A) Eight-week-old B6 mice were intraperitoneally (i.p.) injected LPS (0.8 mg/mouse) with ($n = 15$) or without ($n = 15$) 20 mg 2-DG. Two hours after injection, these mice were intraperitoneally injected 0.8 mg LPS. Survival was monitored for 4 days and analyzed by the Kaplan–Meier method; data were compared between the two groups using the Log-rank (Mantel-Cox) test. $p < .0001$. (B) Two hours after LPS injection as described in (A), serum concentrations of interleukin (IL)-6 and tumor necrosis factor (TNF)- α were measured by ELISAs. Results were analysed using one-way ANOVA followed by Tukey's post hoc test. $****p < .0001$, $***p < .001$, and $*p < .05$. Graphs are presented as the mean \pm s.d. ($n = 6$). (C) Quantitative real-time PCR analysis of monocyte chemoattractant protein-1 (MCP-1), 10 kDa interferon-gamma-induced protein (IP-10), and tumor necrosis factor (TNF)- α mRNAs in left lung tissue 2 days after LPS injection as described in (A). Significant differences were determined using the unpaired two-tailed t-test. $****p < .0001$ and $***p < .001$. (D) Mice were injected i.p. ($n = 3$) with or without 20 mg 2-DG and 100 mg/kg methylprednisolone (mPSL). Subsequently, 10 mg/kg LPS was injected intratracheally. Two days after LPS injection, histological sections of the left lung (Mock, LPS intratracheally injected, LPS+2DG treated, LPS+mPSL treated, and LPS+2DG+mPSL treated) were stained with haematoxylin and eosin (left panel, $\times 2$ and $\times 20$) and with the anti-F4/80 antibody (right panel, $\times 2$ and $\times 20$). Experiments were repeated three times independently with similar results. (E) LPS-induced lung edema as described in (D). Results were analysed using one-way ANOVA followed by Tukey's post hoc test. $****p < .0001$, $**p < .01$, and $*p < .05$. (F) Quantitative real-time PCR analysis of MCP-1 and IP-10 mRNAs in left lung tissue 2 days after LPS injection as described in (D). Results were analysed using one-way ANOVA followed by Tukey's post hoc test. $****p < .0001$, $***p < .001$, $**p < .01$, and $*p < .05$

severe cytokine-related diseases that require hospitalization, such as severe cytokine storms and ARDS. We also showed that 2-DG was effective for the treatment of inflammatory bowel disease and rheumatoid arthritis when administered at a high dose. In addition, another glycoprotein inhibitor, tunicamycin, also effectively suppressed colonic tissue destruction and macrophage infiltration related to DSS-induced inflammation in mice (Figure S8), but its high cytotoxicity makes it difficult to use for therapy. Therefore, it will be necessary to develop glycosylation inhibitors that are effective at lower doses after oral administration. In addition, marked changes in cellular metabolism also alter the phenotype of macrophages: M1 macrophages were shown to be dependent on glycolysis.⁶² Therefore, the inhibition of glycolysis by 2-DG might partly affect the activity of these cells. Further analysis is needed to clarify this issue. Furthermore, in this study, we focused on proinflammatory cytokines, especially IL-6 and TNF- α , but to clarify the overall anti-inflammatory effects of 2-DG, it will be important to examine other proinflammatory cytokines and anti-inflammatory cytokines such as IL-10, whose receptor has been reported to be highly glycosylated.⁶³

Glucocorticoids are currently considered the standard of care for patients with severe COVID-19.¹² However, glucocorticoid therapy in patients with severe COVID-19-related ARDS is associated with increased mortality and delayed viral clearance, which suggests that treatment timing, dosage, and COVID-19 severity determine the outcomes of immunomodulatory therapies.⁶⁴ In the present study, we found that glucocorticoids inhibited LPS-induced pulmonary infiltration, lung edema, and the expression of chemokines relevant to COVID-19. Similar effects were observed following 2-DG administration and combined therapy with glucocorticoids and 2-DG almost completely suppressed these effects. We believe that the small number of animals used in this study may have been a limitation. However, considering the effects of 2-DG on the inflammatory disease models, a therapeutic effect on LPS pneumonia is conceivable. Although detailed analysis of the immunomodulatory effect of 2-DG has not been performed, our results suggest that 2-DG alone or in combination with glucocorticoids may be effective for treatment of

severe COVID-19. Glucocorticoid is also used for treatment of IBD and rheumatoid arthritis.^{65,66} In the present study, although we did not investigate the combined effect of 2-DG on glucocorticoid treatment in our model mice, the results of LPS pneumonia suggest that these models may provide synergistic therapeutic effects and reduced glucocorticoid use. We believe it is necessary to analyse this aspect in the future. Moreover, because the present study mainly analysed the effect of 2-DG on inflammatory disease models, we believe that a detailed analysis of the 2-DG dose response in these mice should be performed in the future for clinical application. Because the actual efficacy against COVID-19 is still speculative, future research will be required to elucidate the potential clinical application of glycosylation agents, including 2-DG.

While anti-proinflammatory cytokine therapies are clinically effective, such as engineered antibodies and soluble cytokine receptors, these protein therapies require multiple injections and are quite expensive, which hinder their use as the primary choice to treat various inflammatory diseases.^{28,67} In practical terms, orally bioavailable, easy-to-synthesize drugs directed against diverse proinflammatory cytokine systems would be preferable. In this regard, 2-DG is a promising anti-inflammatory compound, although a disadvantage is the high dose required for activity. Development of further derivatives may result in increased efficacies and fewer adverse effects. Related compounds with more specific inhibitory effects on receptor N-glycosylation and fewer effects on glycolysis would meet such a requirement.

ETHICS STATEMENT

The animal experiment protocol was approved by the Ethics Committee on Animal Experiments of Nippon Medical School (ethics approval number 21–185, 22–115, 22–140, 23–022, 23–184, 23–186, 24–049, 24–143, 27–126, and 2020–082).

ACKNOWLEDGEMENTS

We are grateful to Keiko Kawauchi, Yoshinori Abe, Wataru Nakajima, and Tomio Yabe for their helpful suggestions and Miho Kawagoe, Hiroko Hiroike, Toshimi Takatera, Yumi Asano, and Seiko Egawa for

technical support. This study was supported by Grants-in-Aid from the Ministry of Education, Culture, Sports, Science and Technology of Japan and the Uehara Memorial Foundation. We thank Mitchell Arico and J. Ludovic Croxford, PhD, from Edanz (<https://jp.edanz.com/ac>) for editing a draft of this manuscript.

DISCLOSURE

The authors declare no conflict of interest.

AUTHOR CONTRIBUTION

N.T. conceived and designed the research; I.U., M.K., A.T., and M.O. performed the experiments; I.U., S.H., Z.N., S.T., and N.T. analyzed data; N.T. and I.U. interpreted the results; I.U. prepared the figures; N.T. and I.U. drafted the manuscript. All authors approved the final version of manuscript.

DECLARATION OF TRANSPARENCY AND SCIENTIFIC RIGOR

This declaration acknowledges that this paper adheres to the principles for transparent reporting and scientific rigor of preclinical research as stated in the BJP guidelines for design and analysis, immunoblotting, and animal experimentation, and as recommended by funding agencies, publishers, and other organizations engaged with supporting research.

PERMISSION TO REPRODUCE MATERIAL FROM OTHER SOURCES

No reproduced material from other sources was present in this study.

DATA AVAILABILITY STATEMENT

The data that support the findings of this study are available from the corresponding author upon reasonable request. Some data may not be made available because of privacy or ethical restrictions.

ORCID

Nobuyuki Tanaka  <https://orcid.org/0000-0002-6373-2220>

REFERENCES

- Medzhitov R. Origin and physiological roles of inflammation. *Nature*. 2008;454(7203):428-435. doi:10.1038/nature07201
- Takeuchi O, Akira S. Pattern recognition receptors and inflammation. *Cell*. 2010;140(6):805-820. doi:10.1016/j.cell.2010.01.022
- Reddick LE, Alto NM. Bacteria fighting back: how pathogens target and subvert the host innate immune system. *Mol Cell*. 2014;54(2):321-328. doi:10.1016/j.molcel.2014.03.010
- Turner MD, Nedjai B, Hurst T, Pennington DJ. Cytokines and chemokines: at the crossroads of cell signalling and inflammatory disease. *Biochim Biophys Acta*. 2014;1843(11):2563-2582. doi:10.1016/j.bbamcr.2014.05.014
- Chan AC, Carter PJ. Therapeutic antibodies for autoimmunity and inflammation. *Nat Rev Immunol*. 2010;10(5):301-316. doi:10.1038/nri2761
- Kang S, Tanaka T, Narazaki M, Kishimoto T. Targeting interleukin-6 signaling in clinic. *Immunity*. 2019;50(4):1007-1023. doi:10.1016/j.immuni.2019.03.026
- Brenner D, Blaser H, Mak TW. Regulation of tumour necrosis factor signalling: live or let die. *Nat Rev Immunol*. 2015;15(6):362-374. doi:10.1038/nri3834
- Neurath MF. Current and emerging therapeutic targets for IBD. *Nat Rev Gastroenterol Hepatol*. 2017;14(5):269-278. doi:10.1038/nrgastro.2016.208
- Cavalli G, Dinarello CA. Treating rheumatological diseases and comorbidities with interleukin-1 blocking therapies. *Rheumatology (Oxford)*. 2015;54(12):2134-2144. doi:10.1093/rheumatology/kev269
- Huang C, Wang Y, Li X, et al. Clinical features of patients infected with 2019 novel coronavirus in Wuhan. *China. Lancet*. 2020;395(10223):497-506. doi:10.1016/S0140-6736(20)30183-5
- Walls AC, Park YJ, Tortorici MA, Wall A, McGuire AT, Veesler D. Structure, function, and antigenicity of the SARS-CoV-2 spike glycoprotein. *Cell*. 2020;183(6):1735. doi:10.1016/j.cell.2020.11.032
- Berlin DA, Gulick RM, Martinez FJ. Severe Covid-19. *N Engl J Med*. 2020;383(25):2451-2460. doi:10.1056/NEJMcp2009575
- Fajgenbaum DC, June CH. Cytokine Storm. *N Engl J Med*. 2020;383(23):2255-2273. doi:10.1056/NEJMra2026131
- Wang K, Qiu Z, Liu J, et al. Analysis of the clinical characteristics of 77 COVID-19 deaths. *Sci Rep*. 2020;10(1):16384. doi:10.1038/s41598-020-73136-7
- Buckley LF, Wohlford GF, Ting C, et al. Role for anti-cytokine therapies in severe coronavirus disease 2019. *Crit Care Explor*. 2020;2(8):e0178. doi:10.1097/CCE.0000000000000178
- Garbers C, Heink S, Korn T, Rose-John S. Interleukin-6: designing specific therapeutics for a complex cytokine. *Nat Rev Drug Discov*. 2018;17(6):395-412. doi:10.1038/nrd.2018.45
- Chames P, Van Regenmortel M, Weiss E, Baty D. Therapeutic antibodies: successes, limitations and hopes for the future. *Br J Pharmacol*. 2009;157(2):220-233. doi:10.1111/j.1476-5381.2009.00190.x
- Kishimoto T. Interleukin-6: from basic science to medicine—40 years in immunology. *Annu Rev Immunol*. 2005;23:1-21. doi:10.1146/annurev.immunol.23.021704.115806
- Hoebke K, Jiang Z, Tabeta K, et al. Genetic analysis of innate immunity. *Adv Immunol*. 2006;91:175-226.
- Domscheit H, Hegeman MA, Carvalho N, Spieth PM. Molecular dynamics of lipopolysaccharide-induced lung injury in rodents. *Front Physiol*. 2020;11:36. doi:10.3389/fphys.2020.00036
- Kawauchi K, Araki K, Tobiume K, Tanaka N. p53 regulates glucose metabolism through an IKK-NF- κ B pathway and inhibits cell transformation. *Nat Cell Biol*. 2008;10(5):611-618. doi:10.1038/ncb1724
- Chassaing B, Aitken JD, Malleshappa M, Vijay-Kumar M. Dextran sulfate sodium (DSS)-induced colitis in mice. *Curr Protoc Immunol*. 2014;104(1):11-15. doi:10.1002/0471142735.im1525s104
- Ueyama H, Okano T, Orita K, et al. Local transplantation of adipose-derived stem cells has a significant therapeutic effect in a mouse model of rheumatoid arthritis. *Sci Rep*. 2020;10(1):3076. doi:10.1038/s41598-020-60041-2
- Cai X, Chen Y, Xie X, Yao D, Ding C, Chen M. Astaxanthin prevents against lipopolysaccharide-induced acute lung injury and sepsis via inhibiting activation of MAPK/NF- κ B. *Am J Transl Res*. 2019;11(3):1884-1894. Retrieved from <https://www.ncbi.nlm.nih.gov/pubmed/30972212>
- Harding SD, Sharman JL, Faccenda E, et al. The IUPHAR/BPS Guide to PHARMACOLOGY in 2018: updates and expansion to encompass the new guide to IMMUNOPHARMACOLOGY. *Nucleic Acids Res*. 2018;46(D1):D1091-D1106. doi:10.1093/nar/gkx1121
- Alexander SPH, Fabbro D, Kelly E, et al. THE CONCISE GUIDE TO PHARMACOLOGY 2021/22: Catalytic receptors. *Br J Pharmacol*. 2021;178(Suppl 1):S264-S312. doi:10.1111/bph.15541
- Alexander SPH, Fabbro D, Kelly E, et al. THE CONCISE GUIDE TO PHARMACOLOGY 2019/20: Enzymes. *Br J Pharmacol*. 2019;176(Suppl 1):S297-S396. doi:10.1111/bph.14752

28. Dinarello CA. Anti-inflammatory agents: present and future. *Cell*. 2010;140(6):935-950. doi: 10.1016/j.cell.2010.02.043
29. Kapoor M, Martel-Pelletier J, Lajeunesse D, Pelletier JP, Fahmi H. Role of proinflammatory cytokines in the pathophysiology of osteoarthritis. *Nat Rev Rheumatol*. 2011;7(1):33-42. doi:10.1038/nrrheum.2010.196
30. Nishimoto N, Kishimoto T. Interleukin 6: from bench to bedside. *Nat Clin Pract Rheumatol*. 2006;2(11):619-626. doi:10.1038/ncprheum0338
31. Murray PJ. The JAK-STAT signaling pathway: input and output integration. *J Immunol*. 2007;178(5):2623-2629. doi:10.4049/jimmunol.178.5.2623
32. Hibi M, Murakami M, Saito M, Hirano T, Taga T, Kishimoto T. Molecular cloning and expression of an IL-6 signal transducer, gp130. *Cell*. 1990;63(6):1149-1157. doi:10.1016/0092-8674(90)90411-7
33. Saito M, Yoshida K, Hibi M, Taga T, Kishimoto T. Molecular cloning of a murine IL-6 receptor-associated signal transducer, gp130, and its regulated expression in vivo. *J Immunol*. 1992;148(12):4066-4071. Retrieved from: http://www.ncbi.nlm.nih.gov/entrez/query.fcgi?cmd=Retrieve&db=PubMed&dopt=Citation&list_uids=1602143
34. Fan JQ, Lee YC. Detailed studies on substrate structure requirements of glycoamidases A and F. *J Biol Chem*. 1997;272(43):27058-27064. Retrieved from: http://www.ncbi.nlm.nih.gov/entrez/query.fcgi?cmd=Retrieve&db=PubMed&dopt=Citation&list_uids=9341145
35. Yanagisawa M, Yu RK. N-glycans modulate the activation of gp130 in mouse embryonic neural precursor cells. *Biochem Biophys Res Commun*. 2009;386(1):101-104. doi:10.1016/j.bbrc.2009.05.132
36. Datema R, Schwarz RT. Interference with glycosylation of glycoproteins. Inhibition of formation of lipid-linked oligosaccharides in vivo. *Biochem J*. 1979;184(1):113-123. Retrieved from: http://www.ncbi.nlm.nih.gov/entrez/query.fcgi?cmd=Retrieve&db=PubMed&dopt=Citation&list_uids=534512
37. Kurtoglu M, Gao N, Shang J, et al. Under normoxia, 2-deoxy-D-glucose elicits cell death in select tumor types not by inhibition of glycolysis but by interfering with N-linked glycosylation. *Mol Cancer Ther*. 2007;6(11):3049-3058. doi:10.1158/1535-7163.MCT-07-0310
38. Soga T, Baran R, Suematsu M, et al. Differential metabolomics reveals ophthalmic acid as an oxidative stress biomarker indicating hepatic glutathione consumption. *J Biol Chem*. 2006;281(24):16768-16776. doi:10.1074/jbc.M601876200
39. Maeda Y, Kinoshita T. Dolichol-phosphate mannose synthase: structure, function and regulation. *Biochim Biophys Acta*. 2008;1780(6):861-868. doi:10.1016/j.bbagen.2008.03.005
40. Gerhartz C, Dittrich E, Stoyan T, et al. Biosynthesis and half-life of the interleukin-6 receptor and its signal transducer gp130. *Eur J Biochem*. 1994;223(1):265-274. Retrieved from: http://www.ncbi.nlm.nih.gov/entrez/query.fcgi?cmd=Retrieve&db=PubMed&dopt=Citation&list_uids=8033901
41. Waetzig GH, Chalaris A, Rosenstiel P, et al. N-linked glycosylation is essential for the stability but not the signaling function of the interleukin-6 signal transducer glycoprotein 130. *J Biol Chem*. 2010;285(3):1781-1789. doi:10.1074/jbc.M109.075952
42. Strober W, Fuss IJ. Proinflammatory cytokines in the pathogenesis of inflammatory bowel diseases. *Gastroenterology*. 2011;140(6):1756-1767. doi:10.1053/j.gastro.2011.02.016
43. Biswas P, Delfanti F, Bernasconi S, et al. Interleukin-6 induces monocyte chemotactic protein-1 in peripheral blood mononuclear cells and in the U937 cell line. *Blood*. 1998;91(1):258-265. Retrieved from http://www.ncbi.nlm.nih.gov/entrez/query.fcgi?cmd=Retrieve&db=PubMed&dopt=Citation&list_uids=9414293
44. Iizuka Y, Okuno T, Saeki K, et al. Protective role of the leukotriene B4 receptor BLT2 in murine inflammatory colitis. *FASEB J*. 2010;24(12):4678-4690. doi:10.1096/fj.10-165050
45. Lara-Villoslada F, Debras E, Nieto A, et al. Oligosaccharides isolated from goat milk reduce intestinal inflammation in a rat model of dextran sodium sulfate-induced colitis. *Clin Nutr*. 2006;25(3):477-488. doi:10.1016/j.clnu.2005.11.004
46. Hata H, Sakaguchi N, Yoshitomi H, et al. Distinct contribution of IL-6, TNF-alpha, IL-1, and IL-10 to T cell-mediated spontaneous autoimmune arthritis in mice. *J Clin Invest*. 2004;114(4):582-588. doi:10.1172/JCI21795
47. Yoshitomi H, Sakaguchi N, Kobayashi K, et al. A role for fungal beta-glucans and their receptor Dectin-1 in the induction of autoimmune arthritis in genetically susceptible mice. *J Exp Med*. 2005;201(6):949-960. doi:10.1084/jem.20041758
48. Kim H, Baumann H. The carboxyl-terminal region of STAT3 controls gene induction by the mouse haptoglobin promoter. *J Biol Chem*. 1997;272(23):14571-14579. Retrieved from: http://www.ncbi.nlm.nih.gov/entrez/query.fcgi?cmd=Retrieve&db=PubMed&dopt=Citation&list_uids=9169415
49. Malle E, Sodin-Semrl S, Kovacevic A. Serum amyloid A: an acute-phase protein involved in tumour pathogenesis. *Cell Mol Life Sci*. 2009;66(1):9-26. doi:10.1007/s00018-008-8321-x
50. Kany S, Vollrath JT, Relja B. Cytokines in inflammatory disease. *Int J Mol Sci*. 2019;20(23):6008. doi:10.3390/ijms20236008
51. Vallabhapurapu S, Karin M. Regulation and function of NF-kappaB transcription factors in the immune system. *Annu Rev Immunol*. 2009;27:693-733. doi:10.1146/annurev.immunol.021908.132641
52. Mosser DM, Edwards JP. Exploring the full spectrum of macrophage activation. *Nat Rev Immunol*. 2008;8(12):958-969. doi:10.1038/nri2448
53. Zhong C, Li P, Argade S, et al. Inhibition of protein glycosylation is a novel pro-angiogenic strategy that acts via activation of stress pathways. *Nat Commun*. 2020;11(1):6330. doi:10.1038/s41467-020-20108-0
54. Mangalmurti N, Hunter CA. Cytokine storms: understanding COVID-19. *Immunity*. 2020;53(1):19-25. doi:10.1016/j.immuni.2020.06.017
55. Costela-Ruiz VJ, Illescas-Montes R, Puerta-Puerta JM, Ruiz C, Melguizo-Rodriguez L. SARS-CoV-2 infection: the role of cytokines in COVID-19 disease. *Cytokine Growth Factor Rev*. 2020;54:62-75. doi:10.1016/j.cytogfr.2020.06.001
56. Vassiliou AG, Kotanidou A, Dimopoulou I, Orfanos SE. Endothelial damage in acute respiratory distress syndrome. *Int J Mol Sci*. 2020;21(22):8793. doi:10.3390/ijms21228793
57. Siewert E, Muller-Esterl W, Starr R, Heinrich PC, Schaper F. Different protein turnover of interleukin-6-type cytokine signalling components. *Eur J Biochem*. 1999;265(1):251-257. doi:10.1046/j.1432-1327.1999.00719.x
58. Raez LE, Papadopoulos K, Ricart AD, et al. A phase I dose-escalation trial of 2-deoxy-D-glucose alone or combined with docetaxel in patients with advanced solid tumors. *Cancer Chemother Pharmacol*. 2013;71(2):523-530. doi:10.1007/s00280-012-2045-1
59. Pajak B, Siwiak E, Sołtyka M, et al. 2-Deoxy-d-glucose and its analogs: from diagnostic to therapeutic agents. *Int J Mol Sci*. 2020;21(1):234. doi:10.3390/ijms21010234
60. Uehara I, Tanaka N. Role of p53 in the regulation of the inflammatory tumor microenvironment and tumor suppression. *Cancers (Basel)*. 2018;10(7):219. doi:10.3390/cancers10070219
61. Nair AB, Jacob S. A simple practice guide for dose conversion between animals and human. *J Basic Clin Pharm*. 2016;7(2):27-31. doi: 10.4103/0976-0105.177703
62. Viola A, Munari F, Sanchez-Rodriguez R, Scolaro T, Castegna A. The metabolic signature of macrophage responses. *Front Immunol*. 2019;10:1462. doi:10.3389/fimmu.2019.01462
63. Tan JC, Braun S, Rong H, et al. Characterization of recombinant extracellular domain of human interleukin-10 receptor. *J Biol Chem*. 1995;270(21):12906-12911. doi:10.1074/jbc.270.21.12906

64. Matthay MA, Wick KD. Corticosteroids, COVID-19 pneumonia, and acute respiratory distress syndrome. *J Clin Invest.* 2020;130(12):6218-6221. doi:10.1172/JCI143331
65. Bruscoli S, Febo M, Riccardi C, Migliorati G. Glucocorticoid therapy in inflammatory bowel disease: mechanisms and clinical practice. *Front Immunol.* 2021;12:691480. doi:10.3389/fimmu.2021.691480
66. Buttgerit F. Views on glucocorticoid therapy in rheumatology: the age of convergence. *Nat Rev Rheumatol.* 2020;16(4):239-246. doi:10.1038/s41584-020-0370-z
67. Wailoo AJ, Bansback N, Brennan A, Michaud K, Nixon RM, Wolfe F. Biologic drugs for rheumatoid arthritis in the Medicare program: a cost-effectiveness analysis. *Arthritis Rheum.* 2008;58(4):939-946. doi:10.1002/art.23374

SUPPORTING INFORMATION

Additional supporting information may be found in the online version of the article at the publisher's website.

How to cite this article: Uehara I, Kajita M, Tanimura A, et al. 2-Deoxy-D-glucose induces deglycosylation of proinflammatory cytokine receptors and strongly reduces immunological responses in mouse models of inflammation. *Pharmacol Res Perspect.* 2022;10:e00940. doi:[10.1002/prp2.940](https://doi.org/10.1002/prp2.940)